# Monolithic Pyroelectric Infrared Sensor Array with Porous $SiO_2$ Film

Xiang-Yu SUN[1,a], Wen-Bo LUO[1,b,*], Xin-Qiang PAN[1,c], Xiao-Yuan BAI[1,d], Jia MENG[1,e], Yao SHUAI[1,f], Chuan-Gui WU[1,g]

[1]State Key Laboratory of Electronic Thin Films and Integrated Devices, University of Electronic Science and Technology of China, Chengdu 610054, P. R. China

[a]xiangyu_s@126.com, [b]luowb@uestc.edu.cn, [c]pan_x_q@sina.com, [d]xynbai@126.com, [e]mjuestc@sina.com, [f]yshuai@uestc.edu.cn, [g]cgwu@uestc.edu.cn

[*]Corresponding author

**Keywords:** Porous thermal Insulator, Dense $SiO_2$ film, Property uniformity

**Abstract.** A simple method to fabricate pyroelectric sensors array using standard semiconductor process on Silicon substrate was investigated. 600 nm porous $SiO_2$ film was prepared by spin coating, working as ultra-thin thermal insulator. Good insulation property was achieved owing to its extremely low thermal conductance. A dense $SiO_2$ layer was made above porous film and provided a smooth surface for sensor fabrication process. Square sensor units of five different sizes from 0.01 $mm^2$ to 2.25 $mm^2$ were produced by photolithography and wet etching. The pyroelectric coefficients of these units were in the range of $2.5\times10^{-9}$ $Ccm^{-2}K^{-1}$ to $3.5\times10^{-9}$ $Ccm^{-2}K^{-1}$. Different sensor units showed similar infrared detective performance at frequency range from 5 Hz to 100 Hz. The excellent directivities were capable for applications of next generation infrared array detector.

## 1. Introduction

Pyroelectric infrared detector is wildly used in many fields such as energy detection, thermometer, gas detection and motion detection [1-4], owing to its high sensitivity, high reliability, low cost and low power consumption. Recent years, in addition, there is a growing demand of infrared imaging devices for military and civil uses [5], which require high cell density and uniform detective performance. Therefore, research on infrared array sensor becomes a hotspot [6].

As is known to all, a typical pyroelectric infrared sensor is made up of thermal insulator, bottom electrode, pyroelectric material, top electrode and absorbing layer [7]. However, fabrication of infrared sensor array is not as easy as the infrared single-element device. In a sensor array, when the element sizes reduced to micrometer range, thermal crosstalk and noise response could remarkably influence the detective property. In addition, the complex connection arrangement needed to be carefully designed and fabricated. Thus, traditional thermal insulating structures were not applicable. Air gaps of few micrometers were difficult to fabricate using standard MEMS processes, while thermal insulating films such as polyimide contribute too much thermal capacity with thickness of over 10 μm, leading the device to an accuracy-speed dilemma. Quite recently, Porous $SiO_2$ film was used to replace traditional insulating structures, owing to its extremely low thermal conductance of about 0.02 W/mK, which was one order of magnitude lower than that of polyimide film [8]. Porous $SiO_2$ film of 780 nm was successfully fabricated on Silicon substrate in our previous work. This layer performed great thermal insulation property and provided negligible thermal capacity to the whole device. It has also been proved effective to keep the stability and accuracy of infrared detector [9].

However, the porous $SiO_2$ structure is fragile and its surface is rough. Electrode patterning is hard to be precisely finished above porous $SiO_2$ film. Moreover, structure collapse would occur during wet etching or other process, which would result in electronic breakover through top and bottom electrodes. This is bad to the application of porous $SiO_2$ film. In this paper, a dense $SiO_2$ film made through sol-gel method was introduced above porous film to improve its surface roughness and enhance the structural strength, which provides a better basement for following patterning and deposition process.

 

Here we proposed a simple way to fabricate infrared sensors with different element sizes on silicon substrate. Porous $SiO_2$ film of 600 nm was used as thermal insulating layer, with 200 nm dense $SiO_2$ capping layer. Pt/Ti electrodes and pyroelectric composite film were deposited by sequence, forming a Metal-Insulator-Metal (MIM) structure.

## 2. Experiment Details

Porous $SiO_2$ aerogel film was fabricated on 100 $mm^2$ p-type silicon substrate. The precursor of Silica alkoxide was prepared using 3-step sol-gel method, catalyzed by HCL, $NH_4OH$ and $NH_4F$ successively [10]. Porous $SiO_2$ film was deposited by spin coating. Thickness was adjusted by changing the spin speed. After aging, solvent exchanging and surface modification, the as-fabricated sample was annealed at 250℃ for few hours before the $SiO_2$ aerogel film was obtained. Dense $SiO_2$ capping layer was deposited right after the formation of porous $SiO_2$ film. This layer was also made using sol-gel method with the precursor of Silica alkoxide. Compact structure was formed during a long time faintly acid catalyzing reaction.

Besides vertical thermal insulation, planar insulation is also crucial for pyroelectric infrared detector. In order to form good insulation, units should be isolated from each other. The sensor array was designed at first that top and bottom electrodes of each unit were overlapped, forming MIM structure. Common ports for top and bottom electrodes were separately designed in order to simplify the polarization process. Element shape was square, and the area were ranging from 0.01 $mm^2$ to 2.25 $mm^2$. Pt/Ti electrodes were deposited by magnetron sputtering. Both electrodes were patterned by photolithography. Patterning of pyroelectric film was carried out using wet etching with the mask of top electrode. In this work, pyroelectric film was a composite of PZT/P(VDF-TrFE), which could be easily dissolved in dimethylacetamide(DMAC).

The surface of sample was observed by Scanning Electron Microscope (SEM). Surface roughness was determined by Atomic Force Microscopy (AFM). The pyroelectric coefficients were measured using dynamic method. The thermal conductance was tested by 3-omega method [11]. Infrared detective properties were measured by a set of infrared testing system including black body radiator (Isotech, R970 blackbody source), preamplifier (model 8153, EG&G, USA), lock-in amplifier (model 7265, EG&G, USA) and oscilloscope (HP54615B).

## 3. Results and discussion

Surface of porous $SiO_2$ film measured by SEM was shown in Fig. 1a. The diameter of pores was about 200 nm. Pores were uniformly located and could be seen at the film surface. The surface SEM image of porous $SiO_2$ film coated by dense $SiO_2$ capping layer was shown in Fig. 1b. It is clearly, pores of porous $SiO_2$ were covered by the capping layer, leaving a shallow pit at each pore position. A great reduction of surface roughness could be observed as well. Bottom electrodes deposited on both porous film and capping layer were also shown in Fig. 1c and Fig. 1d, respectively. AFM was used to further compare the surface roughness between two kinds of surfaces. Results were shown in the insets of Fig. 1c and Fig. 1d, respectively. Rout mean square (RMS) value of surface roughness of the two surfaces were 128 nm and 32 nm respectively. Obviously, a distinct RMS value reduction of almost one order of magnitude has been achieved. Learning from these results, it was crucial that, the inserted dense $SiO_2$ layer not only improved the surface of porous $SiO_2$ film, but also provide a good basement for electrode deposition. Meanwhile, a smooth electrode would largely reduce the difficulty of electrode patterning and other processes of device fabrication.

 

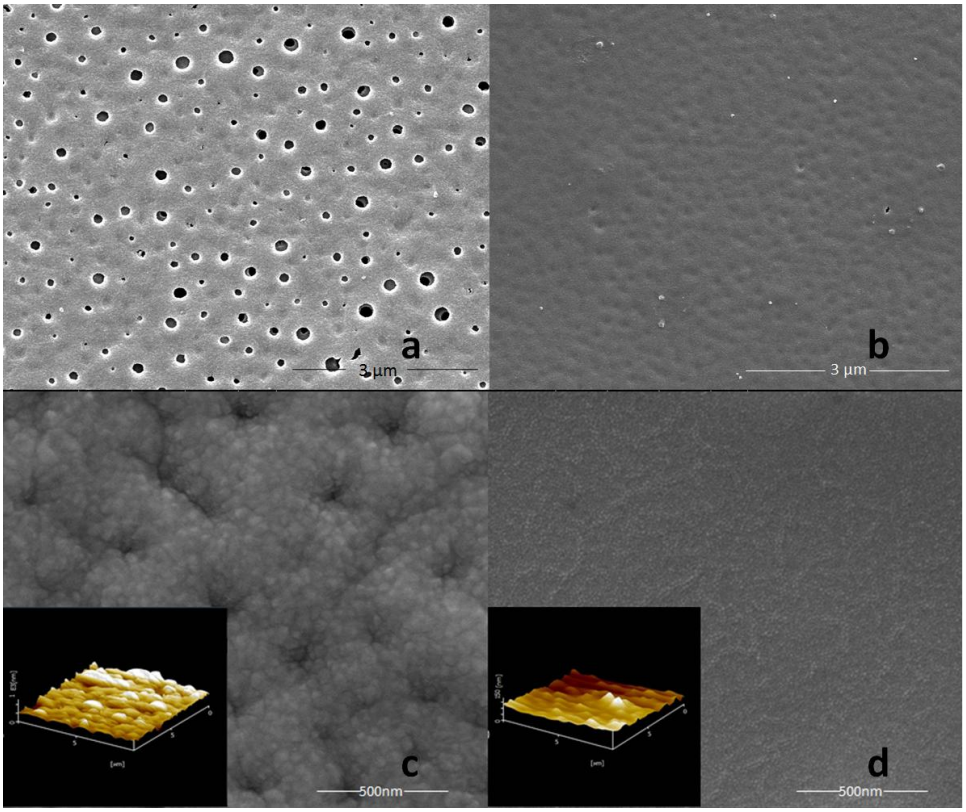


Fig. 1 SEM image of a: surface of porous $SiO_2$ film; b: surface of flat layer; c: surface of bottom electrode on porous $SiO_2$; d: surface of bottom electrode on flat layer. The insets in c and d are the AFM images for the corresponding samples.

Thermal conductivity of porous film and porous film coated by dense $SiO_2$ were $2.78\times10^{-2}$ W/mK and $3.12\times10^{-2}$ W/mK, respectively, measured using 3-ω method [12]. This demonstrated that the very thin dense $SiO_2$ layer didn't contribute much to the thermal conductance. It could then be concluded from all above that the dense $SiO_2$ layer perfectly sealed the pores of porous film and improved its surface flatness. Meanwhile, excellent thermal insulation property was remained.

Etching rate for each concentration of DMAC ethanol solution was shown in table 1. PZT/P(VDF-TrFE) film could be easily dissolved in etchant of concentration ranging from 50% to 100%. However, the composite film couldn't be removed thoroughly unless ultrasonic vibration was applied when concentration of etchant was below 50%. Therefore, 70% DMAC ethanol etchant was optimal due to relatively low etching rate and stable etching effect.

Table 1 etching rate of composite film by different concentrations of DMAC ethanol solution.

| DMAC concentration (%) | Duration (s) | Etching rate (nm/s) |
|---|---|---|
| 100 | 25 | 240 |
| 90 | 36 | 167 |
| 80 | 74 | 81 |
| 70 | 113 | 53 |
| 60 | 240 (with ultrasonic) | / |
| 50 | 540(with ultrasonic) | / |

With dense $SiO_2$ capping layer, the device with different sizes of sensor units was successfully fabricated. SEM image of whole device and its layout were shown in Fig. 2. The area of each unit was 2.25 $mm^2$, 1 $mm^2$, 0.25 $mm^2$, 0.04 $mm^2$ and 0.01 $mm^2$, denoted orderly as A, B, C, D and E, as shown in Fig. 2.

 

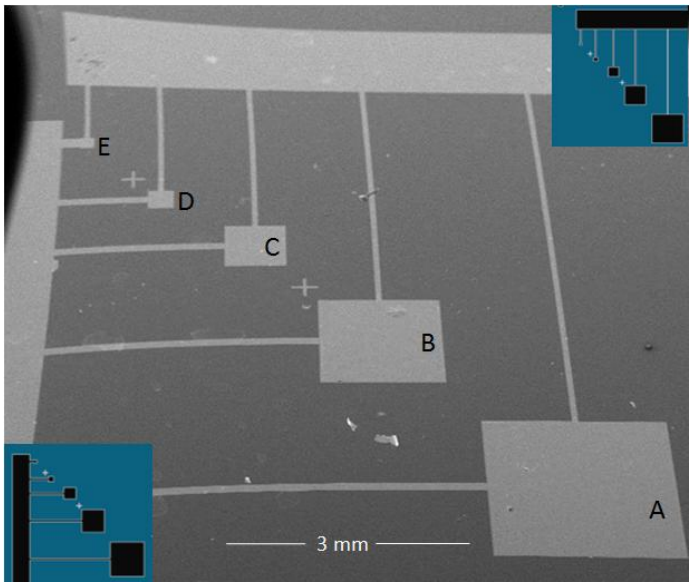


Fig. 2 The layout and SEM image of five infrared sensor units with sizes from 2.25 $mm^2$ to 0.01 $mm^2$, named A, B, C, D and E respectively.

After polarization, the common ports of sensor units were cut off by laser. Thus, electrical properties of each pair of sensor unit could be measured separately. Pyroelectric coefficients were measured by dynamic method under the stimulation of sinusoidal thermal variation. The pyroelectric current of element A under the activation of temperature variations was shown in Fig. 3. The results of other elements revealed that the pyroelectric coefficients were distributed in the range of $2.5\times10^{-9}$ $Ccm^{-2}K^{-1}$ to $3.5\times10^{-9}$ $Ccm^{-2}K^{-1}$. Since sensor units were polarized under the same voltage, the electric field applied on each element was determined by the thickness. This result strongly proved the thickness uniformity of composite film, which should give the credit to the dense $SiO_2$ layer. This value of pyroelectric coefficient was also comparable to those obtained from sensors in our previous work [13], which was around $4\times10^{-9}$ $Ccm^{-2}K^{-1}$.

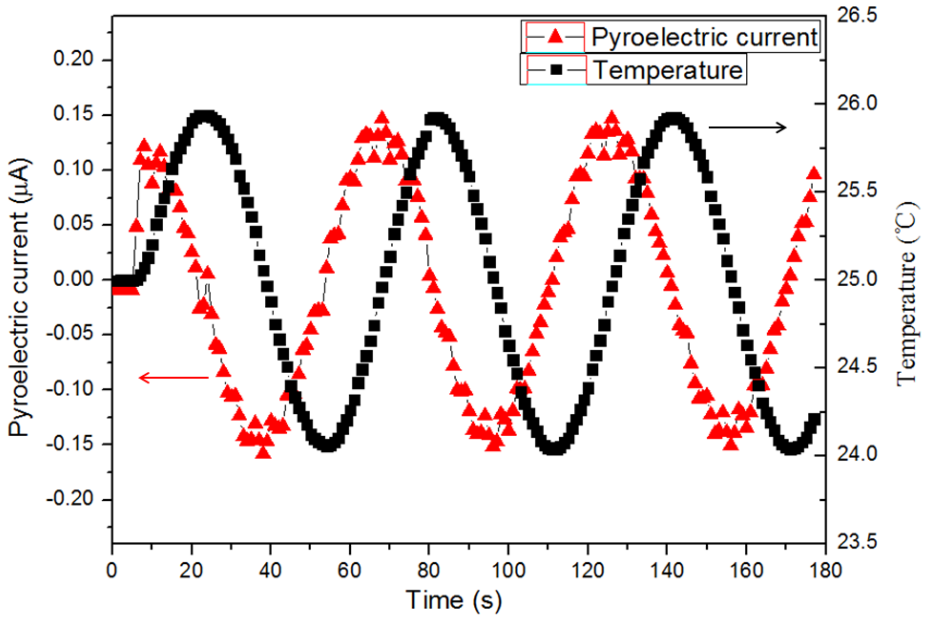


Fig. 3 Pyroelectric current activated under sinusoidal temperature variations with period of 3 min and peak amplitude of 1 ℃.

The infrared detectivities (D*) of each element was calculated by voltage responsivity and noise

 

voltage. Fig. 4 depicted $D^*$ of sensor units from A to D labeled in Fig. 2. According to these results, D* of all these elements were at the range of $7.5\times10^6$ $cmHz^{1/2}W^{-1}$ to $4.9\times10^7$ $cmHz^{1/2}W^{-1}$. The peak value was expected to be even higher according to the D* curves. This demonstrated a good capability of application as infrared detector. However, D* of unit D was comparatively lower than others. This might be caused by its abnormal noise voltage. It is known that the noise voltage consists of intrinsic noise voltage of the device and environmental noise. The intrinsic noise voltage of infrared sensor would decrease along with the decrease of the sensor area. However, environmental noise voltage was constant for each testing system. In unit D, since the environmental noise voltage contributed a big proportion to its integral noise, the calculated D* turned out to be abnormal. For this reason, data of the smallest unit wasn't listed here.

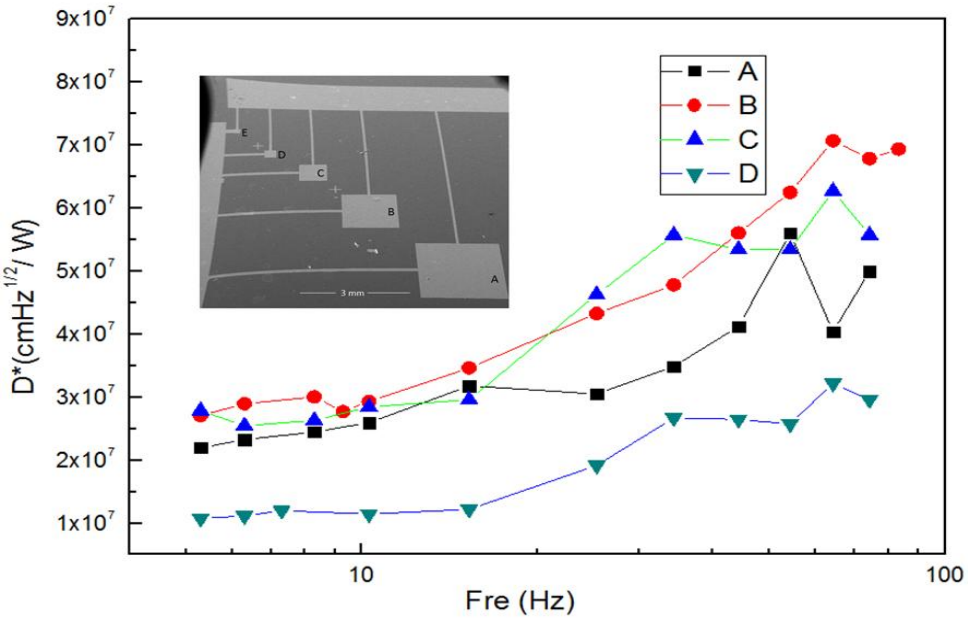


Fig. 4 D* of sensor units with different sizes at various frequencies.

In general, this infrared sensor array is capable for ordinary applications with its competitive detectivity and wide frequency response range. Properties of each unit are similar to each other, which enables the accuracy and stability for infrared imaging. In addition, the simple fabrication process provides a new way for the mass production of infrared sensors.

## 4. Conclusion

Different scales of pyroelectric infrared sensor elements were fabricated by standard integrated manufacturing processes on Si substrate. Porous $SiO_2$ was used as thermal insulation layer. With a dense $SiO_2$ layer, the surface roughness was largely decreased while the high thermal insulation performance of porous $SiO_2$ was remained. Electrodes were patterned by photolithography. PZT/P(VDF-TrFE) composite film was patterned by wet etching method. Pyroelectric coefficients of the sensor units were similar to each other. Detectivities of infrared sensors ranging from $7.5\times10^6$ $cmHz^{1/2}W^{-1}$ to $4.9\times10^7$ $cmHz^{1/2}W^{-1}$ were achieved. The central frequencies were expected to be over 100 Hz. The device showed high compatibility for military and civil uses.

### Acknowledgment

This work has been supported by Sichuan Youth Science and Technology Innovation Research Team Funding (No.2011JTD0006), the National Natural Science Foundation of China (NSFC. 51102037) and the National Natural Science Foundation of China (No. 51402044)

 

## References

[1] A. Odon, Meas. Sci. Rev. 1, 1 (2001).

[2] C. F. Tsai and M. S. Young, Rev. Sci. Instr. 74, 12 (2003).

[3] S. B. Baliga and A. P. Doctor, Proc. SPIE 2366, 39 (1995).

[4] J. Yun and M. H. Song, IEEE Sen. J. 14, 5 (2014).

[5] L. Wang, G. Leedham and S. Y. Cho, IET Comput. Vis. 1, 113 (2007).

[6] R. Yamazaki, A. Obana and M. Kimata, Ele. Comm. JP 96, 2 (2013).

[7] C. G. Wu, X. Y. Sun, J. Meng, W. B. Luo, P. Li, Q. X. Peng, Y. S. Luo and Y. Shuai, Inf. Phys. Technol. 63, 69 (2014).

[8] G. S. Kim, S. H. Hyun, Jour. Non-Crys. Sol. 320, 125–32 (2003).

[9] X. Y. Sun, W. B. Luo, J. Meng, X. Qing, W. Y. Fu, Y. Shuai, and C. G. Wu Sen. Act. A: Phys. 228, 69 (2015).

[10] Y. Q. Xiao, J. Shen, Z. Y. Xie, B. Zhou, G. M. Wu, J. Mater. Sci. Technol. 23, 504 (2007).

[11] H. N. Wang and M. Sen, Int. J. Heat Mass Transf. 52, 2102 (2009).

[12] J. H. Kim, A. Feldman, D. Novotny, J. Appl. Phys. 86, 3959 (1999).

[13] M. Dietze and M. Es-Souni, Sen. Act. A: Phys. 143, 2 (2008).

 